

This document is downloaded from DR-NTU, Nanyang Technological University Library, Singapore.

Title	Indoor contaminant source estimation using a multiple model unscented Kalman filter
Author(s)	Yang, Rong; Foo, Pek Hui; Tan, Peng Yen; See, Elaine Mei Eng; Ng, Gee Wah; Ng, Boon Poh
Citation	Yang, R., Foo, P. H., Tan, P. Y., See, E. M. E., Ng, G. W., & Ng, B. P. (2012). Indoor contaminant source estimation using a multiple model unscented Kalman filter. 2012 15th International Conference on Information Fusion (FUSION), 1854-1859.
Date	2012
URL	http://hdl.handle.net/10220/19822
Rights	© 2012 International Society of Information Fusion. This paper was published in 2012 15th International Conference on Information Fusion (FUSION) and is made available as an electronic reprint (preprint) with permission of International Society of Information Fusion. The paper can be found at the following official URL: http://ieeexplore.ieee.org/xpl/articleDetails.jsp?arnumber=6290526 . One print or electronic copy may be made for personal use only. Systematic or multiple reproduction, distribution to multiple locations via electronic or other means, duplication of any material in this paper for a fee or for commercial purposes, or modification of the content of the paper is prohibited and is subject to penalties under law.

Indoor Contaminant Source Estimation Using a Multiple Model Unscented Kalman Filter

Rong Yang, Pek Hui Foo, Peng Yen Tan,
Elaine Mei Eng See, Gee Wah Ng
DSO National Laboratories
20 Science Park Drive
Singapore 118230
Emails: yrong@dso.org.sg, fpkehui@dso.org.sg,
tpegyen@dso.org.sg, smeiang@dso.org.sg,
ngeewah@dso.org.sg,

Boon Poh Ng
School of EEE
Nanyang Technological University
Blk S2, B2a-05, Nanyang Avenue
Singapore 639798
Email: ebpng@ntu.edu.sg

Abstract—The contaminant source estimation problem is getting increasing importance due to more and more occurrences of sick building syndrome and attacks from covert chemical warfare agents. To monitor a building contamination condition, a number of sensors are connected through a network, and the sensor measurements are sent to a fusion center to estimate contaminant source information. An estimation algorithm is required such that timely actions can be taken to mitigate the adverse effects. This paper proposes a multiple model unscented Kalman filter (MM-UKF) to estimate the contaminant source location, the source emission rate and the release time. A simulation test is conducted on a computer generated three-story building. The results show that the MM-UKF algorithm can achieve real-time estimation.

I. INTRODUCTION

The presence of an airborne contaminant (pollutant) within an indoor environment can put every occupant's health or even life at risk. It is critical for timely action to be taken to mitigate the adverse effects due to contamination. Hence, it is of paramount importance to design tools that can provide real-time information on the contaminant source, via the use of contaminant measurements at a limited number of sensors. The aim of this paper is to develop a methodology to obtain real-time estimation of contaminant source parameters, such as source location, source emission rate, source release time and so on, based on a time sequence of sensor detections in a known building layout.

This is a challenging estimation problem. Firstly, a low computational cost estimation algorithm is required, such that real-time estimation can be performed. Secondly, the transport function on the source location, which we will discuss later, is discontinuous. Thus, the estimation algorithms developed based on continuous functions are not applicable. Before we propose a suitable algorithm, we briefly review the research achievements in the area of contaminant source estimation.

There are two basic approaches for the contamination source estimation problem, namely, the forward approach [1] [2] [3] [4] [5] [6] and the backward approach [7] [8] [9] [10]. The forward approach assumes the transport/migration model, $\mathbf{z} = h(\mathbf{x})$, is known, where \mathbf{z} is the measurement vector, which consists of all the contaminant concentrations detected by the

sensors, \mathbf{x} is the state vector, which contains the contaminant source information, such as source location, emission rate and so on, to be estimated. The forward approach predicts sensor measurements from possible states by the transport model, and finds the most possible state through comparing the detected measurement \mathbf{z} and the predicted measurement $\hat{\mathbf{z}}$. The backward approach obtains the source information from the sensor measurements in the reverse direction. It assumes the backward model $\mathbf{x} = h^{-1}(\mathbf{z})$ is known. Although the backward approach can obtain the source information directly, the backward model $h^{-1}(\cdot)$ is not always available.

In this paper, we focus on the forward approach, which consists of two main components, namely, the transport model and the estimation algorithm. Two commonly used transport methods for indoor contamination are the multi-zone airflow model [11] [12] and the computational fluid dynamics (CFD) model [13] [14]. The multi-zone airflow model generally represents rooms of a building as zones with homogeneous properties and can provide a quick prediction of airflow and contaminant migration. This model can provide fast estimation of contaminant source locations and the relevant source characteristics. Compared to the multi-zone airflow model, the CFD model can provide more spatial and temporal details on airflow and contaminant migration. However, it would not be practical to use a CFD model in real-world scenario simulation, due to the high computational complexity and cost required. We select the multi-zone airflow model in this paper.

The forward estimation algorithms can be categorized into two classes, namely, the optimization approach and the Bayesian approach. The optimization approach [1] [2] [3] [4] [5] [6] is commonly used in groundwater pollution source identification and estimation. This approach obtains the source information through optimizing an objective function on the measurement residual. Linear programming, Newton-Raphson algorithm and regularization method have been suggested to solve this optimization problem. These algorithms often incur high computational costs due to iteration processes. Thus the optimization approach is only applicable to problems with simple $h(\mathbf{x})$. The Bayesian approach is more general

compared to the optimization approach. Bayesian inference is often combined with a Markov chain Monte Carlo (MCMC) sampling procedure to solve the contaminant source estimation problem [15] [16] [17]. An MCMC sampling process initiates one or more Markov chains $\mathbf{x}^1, \dots, \mathbf{x}^m$ with probability $p(\mathbf{x}^1), \dots, p(\mathbf{x}^m)$ based on the prior knowledge, where m is the number of Markov chains in the system. The Monte Carlo process is then carried out for each Markov chain by performing iterative random moves. The Monte Carlo process is terminated when the Markov chains have converged to the posterior distribution. The advantage of the MCMC approach is its applicability to non-Gaussian and nonlinear problems. However, this method also incurs high computational cost as invalid random moves consume a lot of resources.

This paper proposes an MM-UKF algorithm with bounded computational cost to achieve real-time estimation. It is a Kalman-based estimation algorithm. Since a building is normally partitioned into multiple zones, and the source location is represented by the zone index λ , the transport model $h(\cdot)$ becomes a discontinuous function of λ . It is not advisable to estimate a state consisting of an element with discontinuous property using a single model Kalman based filter. Thus, we propose an MM-UKF with multiple UKFs being run in parallel. Each UKF performs estimation of the emission rate ρ and the release time τ conditioned on a distinct zone within the building. The likelihood for each UKF can be computed based on the measurement residual. The source location is then determined by the zone of the UKF with the highest likelihood, and the source emission rate and the release time are the estimation results of the corresponding UKF.

The rest of this paper is organized as follows. Section II introduces the multiple zone airflow model. The model is approximated by a lookup table. Section III formulates the indoor contaminant source estimation problem as a hybrid multiple model estimation problem. Section IV solves the problem by the MM-UKF method. Section V demonstrates the performance of the MM-UKF approach through tests on a simulated 3-story building. Section VI gives a conclusion on this work.

II. MULTIPLE ZONE AIRFLOW MODEL

In the multi-zone airflow model, the building can be first idealized as a complicated interlacing grid system of air-mass flow paths, where nodes represent the zones of the building, and the connections between nodes simulate airflow paths. These airflow paths include flow resistances caused by open or closed doors and windows as well as air leakage through cracks in walls and non-airtight openings. Henceforth, the resulting nodal network resembles an electrical circuit with the airflow paths acting as resistances to flow generated by applied pressure differences. Typically, the airflow rate $F_{j,i}$ from zone j to zone i , is a nonlinear function of the pressure drop along the flow path. Pressure differences can be generated either naturally by the action of wind on the building surface and buoyancy due to differences in density, or mechanically by the action of fans.

The nodal formulation of the network leads to a set of algebraic mass balance equations that must be satisfied simultaneously, while the nonlinearity of the airflow paths necessitates a nonlinear equation solver such as the Newton-Raphson method

$$\xi_k = \xi_{k-1} - \mathbf{J}_{k-1}^{-1} \mathbf{v}_{k-1}, \quad (1)$$

where k is the iteration index, \mathbf{J} represents the Jacobian matrix of residual derivatives, ξ represents the pressure vector and \mathbf{v} represents the flow residual vector.

The multi-zone transport model subsequently captures the transport of contaminants by advection via calculated inter-zone airflows and well-defined mechanical system flows via the mass conservation equation

$$\frac{dm_i}{dt} = -R_i C_i - \sum_j F_{i,j} C_i + \sum_j F_{i,j} (1 - \eta_{j,i}) C_j + G_i, \quad (2)$$

where t represents time, i and j are the zone indices, m_i is the contaminant mass in zone i (kg), R_i is the removal rate in zone i (kg air/s), C_i is the contaminant concentration in zone i (kg/kg air), $F_{i,j}$ is the airflow rate from zone i to zone j (kg air/s), $\eta_{j,i}$ is the filtration efficiency between zone i and zone j , and G_i is the contaminant generation rate in zone i (kg/s).

In this research, we consider instantaneous emission as the emission type. The contaminant generation rate G_i of the instantaneous emission is defined as

$$G_i = \begin{cases} \rho & t = \tau \\ 0 & t > \tau \end{cases}, \quad (3)$$

where τ is the release time, and ρ is the emission rate.

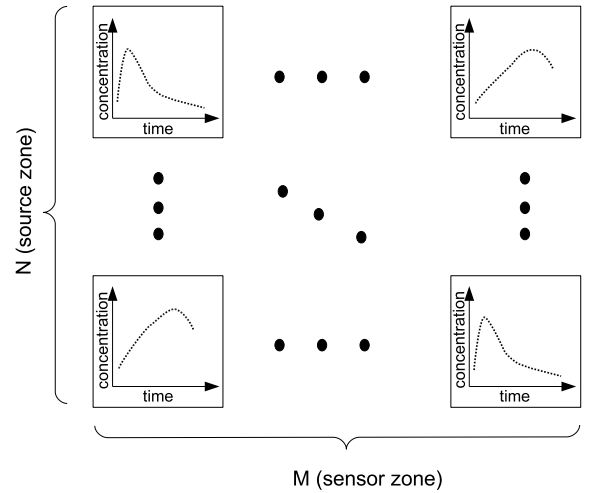


Fig. 1. Lookup table structure. M is the number of sensor zones, and N is the number of zones in the building. Each zone has at most one sensor, i.e. $M \leq N$.

Although the multi-zone airflow model incurs much less computational cost than a CFD model, it may still be too complex for practical implementation. We approximate the multi-zone airflow transport model by a lookup table [15] [16].

The lookup table is built up based on the multi-zone airflow transport model off-line. The structure of the lookup table is shown in Figure 1. It stores concentration value versus time for all possible dispersions from a source zone to a sensor zone. Thus, the size of the table would be $M \times N \times K$, where M is the number of sensors deployed among the zones (each zone has at most one sensor), N is the number of zones in the building, and K is the number of time units in the whole dispersion process.

The emission rates in the lookup table are set to a standard value. If we assume that the resulting concentrations at sensor zones are approximately proportional to the source strength, all possible measurement values can eventually be obtained from the lookup table. This assumption is true for the instantaneous emission.

III. PROBLEM FORMULATION

A dynamic estimation problem can be described by the following equations

$$\mathbf{x}_k = f_{k-1}(\mathbf{x}_{k-1}) + \mathbf{w}_{k-1}, \quad (4)$$

$$\mathbf{z}_k = h_k(\mathbf{x}_k) + \mathbf{r}_k, \quad (5)$$

where \mathbf{x}_k is the state vector which normally consists of the parameters to be estimated, \mathbf{z}_k is the measurement vector, \mathbf{w}_{k-1} is the process noise to compensate the transition model error, and \mathbf{r}_k is the measurement noise; $f_{k-1}(\cdot)$ and $h_k(\cdot)$ are the state transition function and the measurement function respectively.

In our problem, we estimate a single contaminant source with instantaneous emission. The most important parameter to be estimated is the source location, which is represented by the zone index λ . Since λ is discontinuous in the transport function, it cannot be estimated by the algorithms developed based on the continuous function. Thus, we formulate the problem as a hybrid system with multiple hypotheses, and each hypothesis stands for a particular zone. The hybrid system with N hypotheses is constructed as

$$\begin{aligned} \text{Hypothesis}^1 & \begin{cases} \lambda^1 = 1, \\ \mathbf{x}_k^1 = \mathbf{I}_2 \mathbf{x}_{k-1}^1, \\ \mathbf{z}_k = \mathbf{h}_k(\mathbf{x}_k^1, 1) + \mathbf{r}_k, \end{cases} \\ \text{Hypothesis}^2 & \begin{cases} \lambda^2 = 2, \\ \mathbf{x}_k^2 = \mathbf{I}_2 \mathbf{x}_{k-1}^2, \\ \mathbf{z}_k = \mathbf{h}_k(\mathbf{x}_k^2, 2) + \mathbf{r}_k, \end{cases} \\ \vdots & \\ \text{Hypothesis}^N & \begin{cases} \lambda^N = N, \\ \mathbf{x}_k^N = \mathbf{I}_2 \mathbf{x}_{k-1}^N, \\ \mathbf{z}_k = \mathbf{h}_k(\mathbf{x}_k^N, N) + \mathbf{r}_k, \end{cases} \end{aligned} \quad (6)$$

where N is the number of hypotheses in the hybrid system, and it is equal to the number of zones in the building; λ is the source zone index; \mathbf{x}_k^i is the state of hypothesis i , and it is defined as $[\rho^i \ \tau^i]^T$, with ρ^i and τ^i being the source emission rate and the release time of hypothesis i respectively; \mathbf{z}_k is the sensor measurements defined as

$$\mathbf{z}_k = [z_1 \ z_2 \ \cdots \ z_M]^T, \quad (7)$$

where z_i is the contaminant concentration detected by sensor i , $i = 1, \dots, M$, M is the number of sensors deployed. \mathbf{I}_2 is the 2×2 identity matrix, and the process noise \mathbf{w}_{k-1} becomes $\mathbf{0}$ and is ignored in this problem. The transport function $h_k(\cdot)$ is the lookup table, which has been described in Section II.

IV. MULTIPLE MODEL UNSCENTED KALMAN FILTER

We propose a multiple model unscented Kalman filter (MM-UKF) to solve the problem formulated in Section III. The MM-UKF has a total of N UKFs corresponding to N hypotheses run in parallel, and provides N estimation results $\mathbf{x}_k^1, \dots, \mathbf{x}_k^N$, where $\mathbf{x}_k^i = [\rho^i \ \tau^i]^T$. The final result is the state with the highest likelihood. The details of the UKF and the multiple model approach are described in the following subsections.

A. Unscented Kalman filter

A single UKF for one of the hypotheses estimates the local state $\mathbf{x}_k^i = [\rho^i \ \tau^i]^T$ conditioned on $\lambda^i = i$, where $i = 1, \dots, N$.

The unscented Kalman filter [18] [19] uses a set of sample points (also known as ‘‘sigma points’’) to represent the system state probability density function (pdf). These sigma points are transited through the nonlinear transformation functions. The mean and the covariance of the posterior state are computed through the transited sigma points. We select the UKF in this research as it is an efficient nonlinear estimator, and it outperforms the extended Kalman filter in many nonlinear estimation applications [20].

In the UKF, we represent the state pdf by $2n_x + 1$ sigma points χ_k^j and the associated weights W^j , $j = 1, \dots, 2n_x + 1$, where n_x is the state size. In our nonlinear model, $n_x = 2$, and the number of sigma points N_x is 5. Let \mathbf{x}_k^i denote the current state and \mathbf{P}_k^i denote its corresponding covariance for hypothesis i . The χ_k^j and its weight W^j are

$$\chi_k^j = \begin{cases} \mathbf{x}_k^i, & j = 1 \\ \mathbf{x}_k^i + \left(\sqrt{(n_x + \kappa) \mathbf{P}_k^i} \right)_{j-1}, & j \in [2, n_x + 1] \\ \mathbf{x}_k^i - \left(\sqrt{(n_x + \kappa) \mathbf{P}_k^i} \right)_{j-1-n_x}, & j \in [n_x + 2, 2n_x + 1] \end{cases} \quad (8)$$

and

$$W^j = \begin{cases} \frac{\kappa}{n_x + \kappa}, & j = 1 \\ \frac{1}{2(n_x + \kappa)}, & j \in [2, 2n_x + 1] \end{cases} \quad (9)$$

where $(\sqrt{(n_x + \kappa) \mathbf{P}_k^i})_j$ indicates the j th column of the matrix $(\sqrt{(n_x + \kappa) \mathbf{P}_k^i})$, κ is a scalar to determine the spread of sigma points.

The prediction and update steps are then carried out at each cycle. They are described as follows.

$$\mathbf{Z}_k^j = h(\chi_{k-1}^j, j) \quad (10)$$

$$\hat{\mathbf{z}}_k = \sum_{j=1}^{N_x} W^j \mathbf{Z}_k^j \quad (11)$$

$$\mathbf{v}_k = \mathbf{z}_k - \hat{\mathbf{z}}_k \quad (12)$$

$$\mathbf{x}_k^i = \mathbf{x}_{k-1}^i + \mathbf{K}_k \mathbf{v}_k \quad (13)$$

$$\mathbf{P}_k^i = \mathbf{P}_{k-1}^i - \mathbf{K}_k \mathbf{S}_k \mathbf{K}_k^T \quad (14)$$

where

$$N_x = 2n_x + 1 \quad (15)$$

$$\mathbf{K}_k = \mathbf{P}_{xz} \mathbf{S}_k^{-1} \quad (16)$$

$$\mathbf{S}_k = \mathbf{R}_k + \mathbf{P}_{zz} \quad (17)$$

$$\mathbf{P}_{xz} = \sum_{j=1}^{N_x} W^j \tilde{\chi}_k^j (\tilde{\mathbf{Z}}_k^j)^T \quad (18)$$

$$\mathbf{P}_{zz} = \sum_{j=1}^{N_x} W^j \tilde{\mathbf{Z}}_k^j (\tilde{\mathbf{Z}}_k^j)^T \quad (19)$$

$$\tilde{\mathbf{Z}}_k^j = \mathbf{Z}_k^j - \hat{\mathbf{z}}_k \quad (20)$$

$$\tilde{\chi}_k^j = \chi_k^j - \hat{\mathbf{x}}_k \quad (21)$$

The UKF does not require explicit calculation of the Jacobian matrix of the nonlinear state transition equation or the measurement equation. Thus, it is easy for implementation.

B. Multiple model approach

The multiple model estimation approach is widely used in state estimation when model or parameter uncertainty exists. Here, the problem is formulated as a hybrid system. The generic hybrid system can be described as

$$\mathbf{x}_k^i = f_k^i(\mathbf{x}_{k-1}^i) + \mathbf{w}_k, \quad (22)$$

$$\mathbf{z}_k = h_k^i(\mathbf{x}_k^i) + \mathbf{r}_k, \quad (23)$$

where i is the system model index at time k . The models are predetermined in a model set. In our problem, N models representing N possible zones are constructed. Figure 2 illus-

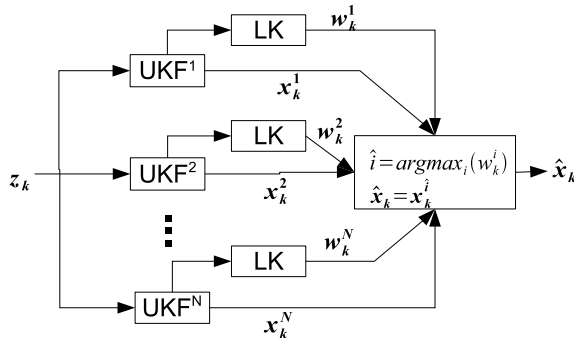


Fig. 2. The structure of the MM-UKF with N models

trates the structure of the multiple model approach formulated for our problem. N UKFs provide N individual estimates, and the LK function computes the likelihood (or weight) for

each model. The final output of the hybrid system $\hat{\mathbf{x}}_k$ is the individual state with the highest weight. The $\hat{\mathbf{x}}_k$ and its error covariance \mathbf{P}_k are

$$\hat{\mathbf{x}}_k = \mathbf{x}_k^{\hat{i}}, \quad (24)$$

$$\mathbf{P}_k = \mathbf{P}_k^{\hat{i}}, \quad (25)$$

where

$$\hat{i} = \arg \max_{i=1:N} w_k^i. \quad (26)$$

If we assume the weighting coefficient w^i is embedded in the measurement sequence, based on the Bayes' rule, the weight for model i can be written as

$$\begin{aligned} w_k^i &= p\{\mu^i | \mathbf{Z}_k\} \\ &= p\{\mu^i | \mathbf{z}_k, \mathbf{Z}_{k-1}\} \\ &= \frac{p\{\mathbf{z}_k | \mathbf{Z}_{k-1}, \mu^i\} p\{\mu^i | \mathbf{Z}_{k-1}\}}{\sum_{j=1}^N p\{\mathbf{z}_k | \mathbf{Z}_{k-1}, \mu^j\} p\{\mu^j | \mathbf{Z}_{k-1}\}} \\ &= \frac{p\{\mathbf{z}_k | \mathbf{Z}_{k-1}, \mu^i\} w_{k-1}^i}{\sum_{j=1}^N p\{\mathbf{z}_k | \mathbf{Z}_{k-1}, \mu^j\} w_{k-1}^j}, \end{aligned} \quad (27)$$

where \mathbf{Z}_k is the measurement sequence up to time k , and is represented as $\{\mathbf{z}_1, \mathbf{z}_2, \dots, \mathbf{z}_k\}$. μ^i is the i th model in the model set. $p\{\mathbf{z}_k | \mathbf{Z}_{k-1}, \mu^i\}$ can be derived from measurement residual \mathbf{v}_k and its covariance \mathbf{S}_k in the UKF estimation of model i , which are defined in (12) and (17) respectively. It is

$$p\{\mathbf{z}_k | \mathbf{Z}_{k-1}, \mu^i\} = \mathcal{N}[\mathbf{v}_k; 0, \mathbf{S}_k], \quad (28)$$

where $\mathcal{N}[\cdot]$ is the white Gaussian function with covariance \mathbf{S}_k .

The algorithm we introduced above is a static MM algorithm. It assumes the models do not switch with time. The static MM algorithm can achieve the optimal solution if the following two assumptions are correct. Firstly, the correct model is in the model set. Secondly, the model does not vary with time. Obviously, the assumptions are true in our problem.

V. SIMULATION RESULTS

The simulation test is conducted for a 3-story building. The floor plan of the building is displayed in Figure 3. It is partitioned into $N = 32$ zones. The links between any two zones indicate there is airflow between them. There are six zones in the building, namely, zones 4, 5, 14, 15, 27 and 28, which are excluded from the simulation study. These zones are negatively pressurized areas, where exhaust fans are installed. Chemicals/contaminants in these zones are expelled from the building instead of being dispersed into the other zones. Some zones in the building belong to low dispersion zones. These zones are located at the end of airflow paths in general. It is difficult for them to disperse chemicals/contaminants to their neighbors. The low dispersion zones in our simulation include zones 22, 24 and 25.

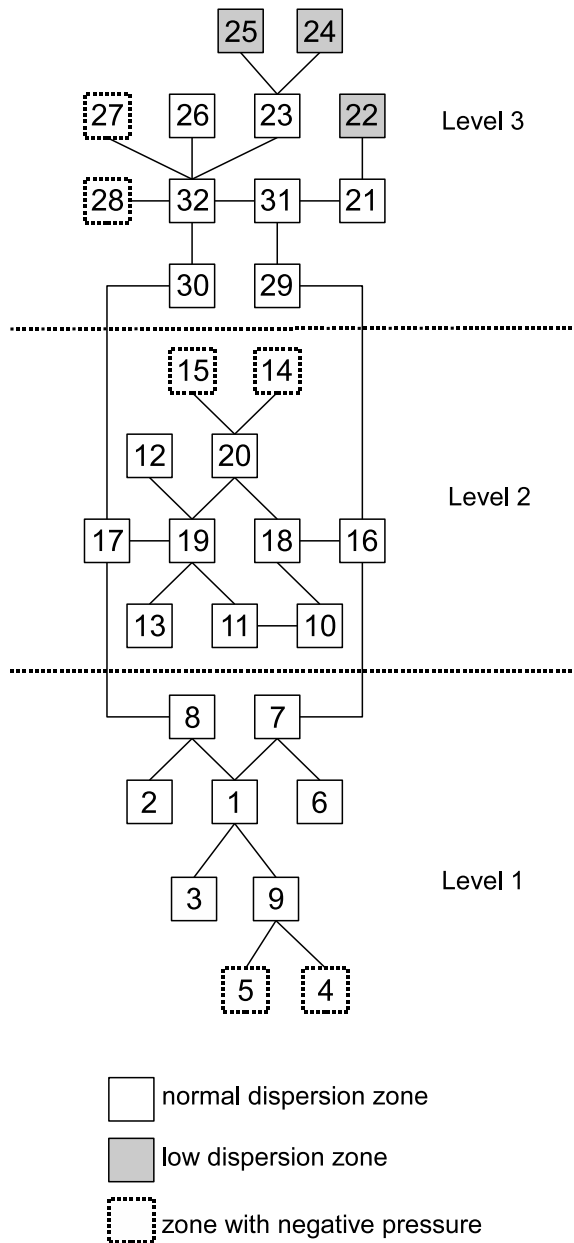


Fig. 3. Floor plan for a 3-story building

A limited number of sensors are deployed among the zones to monitor the building condition. In this simulation, we design two sensor deployments. The first deployment places six sensors in zones 1, 19, 22, 24, 25 and 32. These zones include corridors (zones 1, 19 and 32) and low dispersion zones (zones 22, 24 and 25). The second deployment adds two more sensors in zones 8 and 13, which have similar dispersion pattern to the other zones. The measurements of these sensors are sent to the fusion center for contaminant source estimation at every time cycle with interval $T = 10s$.

In the tests, the emission rate ρ is set to $1kg/s$, and the release time $\tau = 5T$. It means that the contaminant source starts to emit at the 5th time cycle with the instantaneous

emission rate $1kg/s$. The test is carried out on each of the 26 possible zones (exclude six negatively pressurized zones). In each test, a simulator generates the sensor measurements at every time cycle using the lookup table based on ρ and τ for a particular source zone. Since the measurement accuracy of a chemical sensor is decreasing with concentration value, we assume the measurement error is proportional to the measurement value. Thus, the white Gaussian noise with standard deviation of 10% of measurement value is added to the simulated sensor measurement.

The tests focus on the duration that is spent on finding a contaminant source after emission. The number of time cycles is recorded from the release time to the time that the source location is estimated correctly. Here the correct estimation means that the MM-UKF algorithm estimates the source location correctly in three consecutive times. The errors on the emission rate ρ and release time τ are the estimation results at the third correct time. The test results from 50 Monte Carlo runs for the two sensor deployments are shown in Table I and Table II respectively.

TABLE I
MM-UKF PERFORMANCE ON THE 6-SENSOR DEPLOYMENT

zone	duration (T)	error on ρ (kg/s)	error on τ (T)
1*	6	0.029	0.2
19*	5	0.043	0.2
22*	3	0.069	0.4
24*	3	0.046	0.4
25*	3	0.058	0.3
32*	5	0.030	0.2
2	7	0.142	0.2
3	14	0.030	0.1
6	6	0.076	0.2
7	5	0.067	0.3
8	11	0.028	0.1
9	4	0.067	0.2
10	5	0.081	0.2
11	9	0.049	0.2
12	5	0.069	0.2
13	18	0.028	0.2
16	7	0.244	0.3
17	4	0.062	0.3
18	5	0.068	0.2
20	6	0.058	0.3
21	4	0.061	0.3
23	4	0.043	0.2
26	4	0.066	0.3
29	5	0.057	0.2
30	4	0.056	0.3
31	4	0.045	0.3
Avg	6.0	0.064	0.24

* indicates zone with sensor

From the tables, we observe that the contaminant source can be located promptly for the sensor zones. They achieve the fastest speed of $3T$. Since we set a $3T$ buffer for declaring a correct estimation, the MM-UKF algorithm actually finds the correct location at the first time cycle for these sensor zones. It can be seen the performance improved with the 8-sensor deployment. The durations of finding the source for all zones are fewer than $10T$ in the 8-sensor deployment, whereas the longest duration is $18T$ in the 6-sensor deployment. The

TABLE II
MM-UKF PERFORMANCE ON THE 8-SENSOR DEPLOYMENT

zone	duration (T)	error on ρ (kg/s)	error on τ (T)
1*	5	0.040	0.2
8*	3	0.047	0.2
13*	3	0.044	0.3
19*	4	0.039	0.3
22*	3	0.062	0.4
24*	3	0.061	0.3
25*	3	0.066	0.4
32*	5	0.025	0.2
2	4	0.073	0.3
3	8	0.030	0.2
6	5	0.052	0.1
7	5	0.033	0.2
9	4	0.083	0.3
10	5	0.047	0.1
11	9	0.020	0.2
12	4	0.046	0.3
16	7	0.478	0.5
17	4	0.048	0.3
18	5	0.048	0.2
20	6	0.030	0.3
21	4	0.073	0.3
23	4	0.035	0.3
26	4	0.048	0.3
29	5	0.049	0.2
30	4	0.041	0.3
31	4	0.046	0.2
Avg	4.6	0.064	0.27

* indicates zone with sensor

average duration of finding the source reduces from $6.0T$ in the 6-sensor deployment to $4.6T$ in the 8-sensor deployment. The errors on emission rate and release time in the 8-sensor deployment are similar to the 6-sensor deployment, although the durations are shorter.

The computational efficiency is also recorded in the tests. The MM-UKF algorithm completes the estimation process for one time cycle in an average of $12ms$. This is much less than $T = 10s$. Thus, we can conclude that the MM-UKF algorithm can achieve real-time implementation.

VI. CONCLUSION

In this research, an MM-UKF algorithm is proposed for the task of contaminant source estimation in a given indoor environment. A simulation study has been carried out to evaluate the practicability of the proposed approach. The indoor area of interest is a multi-zone environment within a 3-story building. The simulation test results corroborate the feasibility of the MM-UKF algorithm. Generally, the method can achieve accurate estimation of the required contaminant source characteristics (location, emission rate, and release time), and it is real-time implementable.

REFERENCES

[1] S. M. Gorelick, B. Evans, and I. Remson, "Identifying sources of groundwater pollution: An optimization approach," *Water Resources Research*, vol. 19, no. 3, pp. 779–790, 1983.
[2] P. S. Mahar, "Optimal monitoring network and ground water pollution source identification," *Water Resources Planning and Management*, vol. 123, no. 4, pp. 199–207, 1997.

[3] T. H. Skaggs and Z. J. Kabala, "Recovering the release history of a groundwater contaminant," *Water Resources Research*, vol. 30, no. 1, pp. 71–79, 1994.
[4] S. Alapati and Z. J. Kabala, "Recovering the release history of a groundwater contaminant using a non-linear least-squares method," *Hydrological Processes*, vol. 14, no. 6, pp. 1003–1016, 2000.
[5] P. S. Mahar and B. Datta, "Identification of pollution sources in transient groundwater systems," *Water Resources Management*, vol. 14, pp. 209–227, 2000.
[6] —, "Optimal identification of ground-water pollution sources and parameter estimation," *Water Resources Planning and Management*, vol. 127, no. 1, pp. 20–29, 2001.
[7] T. H. Skaggs and Z. J. Kabala, "Recovering the history of a groundwater contaminant plume: method of quasi-reversibility," *Water Resources Research*, vol. 31, pp. 2669–1673, 1995.
[8] J. Atmadja and A. Bagtzoglou, "Groundwater pollution source identification using the backward beam equation method," *Computational Methods for Subsurface Flow and Transport*, 2000, Balkema Publishers, Rotterdam, Netherlands, pp. 397–404.
[9] R. M. Neupauer and J. L. Wilson, "Adjoint method for obtaining backward-in-time location and travel time probabilities of a conservative groundwater contaminant," *Water Resources Research*, vol. 35, pp. 3389–3398, 1999.
[10] —, "Adjoint-derived location and travel time probabilities for a multi-dimensional groundwater system," *Water Resources Research*, vol. 37, pp. 1657–1668, 2000.
[11] A. Schaelin, V. Dorer, J. van der Maas, and A. Moser, "Improvement of multizone model predictions by detailed flow path values from CFD calculation," *ASHRAE Transactions*, vol. 99, no. 2, pp. 709–720, 1993.
[12] A. Musser, "An analysis of combined CFD and multizone IAQ model assembly issues," *ASHRAE Transactions*, vol. 107, no. 1, pp. 371–382, 2001.
[13] P. V. Nielsen, "The selection of turbulence models for prediction of room airflow," *ASHRAE Transactions*, vol. 104, no. 1B, pp. 1119–1127, 1998.
[14] J. D. Spengler and Q. Y. Chen, "Indoor air quality factors in designing a healthy building," *Annual Review of Energy and the Environment*, vol. 25, no. 1B, pp. 567–600, 2000.
[15] F. K. Chow, B. Kosovic, and S. Chan, "Source inversion for contaminant plume dispersion in urban environments using building-resolving simulations," *Proceedings of the 86th American Meteorological Society Annual Meeting*, 2006, Atlanta, Georgia, USA.
[16] —, "Source inversion for contaminant plume dispersion in urban environments using building-resolving simulations," *Journal of Applied Meteorology and Climatology*, vol. 47, no. 6, pp. 1553–1572, 2008.
[17] M. D. Sohn, P. Reynolds, N. Singh, and A. J. Gadgil, "Rapidly locating and characterizing pollutant releases in buildings," *Air and Waste Management Association*, vol. 52, no. 12, pp. 1422–1432, 2002.
[18] S. J. Julier and J. K. Uhlmann, "A new extension of the Kalman filter to nonlinear systems," *In Proceedings of AeroSense: The 11th International Symposium on Aerospace/Defense Sensing, Simulation and Controls*, 1997, Orlando, Florida, USA.
[19] S. J. Julier, J. K. Uhlmann, and H. F. Durrant-Whyte, "A new method for the nonlinear transformation of means and covariances in filters and estimators," *IEEE Transactions on Automatic Control*, vol. 45, no. 3, pp. 477–482, 2000.
[20] S. J. Julier and J. K. Uhlmann, "Unscented filtering and nonlinear estimation," *Proceedings of the IEEE*, vol. 92, no. 3, pp. 401–422, 2004.